Critical heat flux tests on accident tolerant fuel cladding under PWR and BWR conditions

Donghwi Lee [a*], Tiago Augusto Moreira [b], Mark H. Anderson [b]
[a]*Div. of Mechanical System Eng., Jeonbuk National University, 567 Baekje-daero, Deokjin-gu, Jeonju 54896, Korea*
[*]Corresponding authors: dlee462@jbnu.ac.kr (D. Lee)
[b]*Thermal Hydraulics Laboratory, Department of Mechanical Engineering, University of Wisconsin-Madison, 1500 Engineering Drive, ZIP code: 53706, Madison, WI, USA*

1. Introduction

The nuclear reactor needs high-performance cooling methods to cool down the reactor core temperature during the operation. In this regard, flow boiling heat transfer have being used to cool down the reactor core in pressurized water reactors (PWRs) and boiling water reactors (BWRs). There is a crucial factor which means the limitation of allowable heat flux in boiling heat transfer, and it is defined as critical heat flux (CHF). CHF is categorized into two types, dry-out, and departure from nucleate boiling (DNB). Dry-out referred to situations in which a vapor film covered the surface at high vapor quality and DNB referred to situations in which a thin-vapor blanket abruptly covers the surface at low vapor quality(α<0.25). Since those vapor films (dry-out) or thin blankets (DNB) inhibit the liquid supply to the surface, the surface temperature rises rapidly, resulting in a surface failure at CHF. Therefore, CHF tests are necessary to secure the safe operating conditions of BWRs/PWRs.

Zirconium (Zr) alloys have been used as fuel cladding since it has high strength, low neutron cross-section, and high-oxidation resistance at operating condition. However, Zr alloys have a severe problem at the high-temperature: their exothermic reactions above 1200°C. In detail, at temperatures above 1200°C in vapor environmental conditions, Zr generates huge exothermic heat, fgfdestroying the fuel cladding and releasing large amounts of hydrogen gas which can induce an explosion. Therefore, there is a risk of radio-nuclide release due to the explosion of the fuel rod in the event of a loss of coolant accident (LOCA). The Fukushima accident in 2011 was induced by the risks of Zr cladding. Therefore, after the Fukushima accident in 2011, Accident Tolerant Fuel (ATF) concept was demonstrated to solve those problems. The ATF material concept is divided into two strategies. The first strategy is adding chromium coating (metals of low oxidation) to the Zr cladding using cold-spraying or physical vapor deposition (PVD) methods to prevent the explosion at the LOCA. The second strategy is to replace the Zr cladding with FeCrAl alloy which is oxidized with slower rate at high-temperature conditions to remove the risk of explosion at the LOCA. In the previous ATF research, there were many CHF testing research under low-pressure conditions (atmospheric conditions). The results showed that CHF was almost not changed within the 10% range [1,2], but this was not proven in the high-pressure condition (i.e. BWR and PWR conditions)

In this study, Zr, cold-spraying based chromium-coated Zr, and FeCrAl (APMT) were tested in the high-pressure loop of the Thermal Hydraulic Laboratory located at Wiconsin-Madison University. Critical heat flux tests were conducted on the Zr, chromium-coated Zr, and FeCrAl (APMT) under the 10~20 Mpa, 10~60 ℃ subcooling, and 1695~2712kg/m²s mass flux conditions using optical fiber sensors.

2. Methods and Results

2.1 Experimental Apparatus

The Thermal-Hydraulic Laboratory at the University of Wisconsin–Madison (UW-Madison) has a high-pressure flow boiling facility at Stoughton. Before the critical heat flux (CHF) test, UW-Madison and Westinghouse designed the text matrix based on the prototype pressurized water reactor (PWR) conditions. As shown in Fig. 1, CHF tests were conducted in the high-pressure flow boiling heat transfer loop using the single heater rod for the PWR conditions. The length of the heater rod was ~3 m and the heated length was 2 m. A single Heater rod was designed in the Stern Lab which has the cosine profile heater flux with indirect heating. The high-pressure loop can operate in both subcooling and saturated conditions with high pressure of 25 MPa. This high-pressure flow loop can simulate the PWR condition by controlling the inlet quality at the beginning of the heated length. The high-pressure flow loop

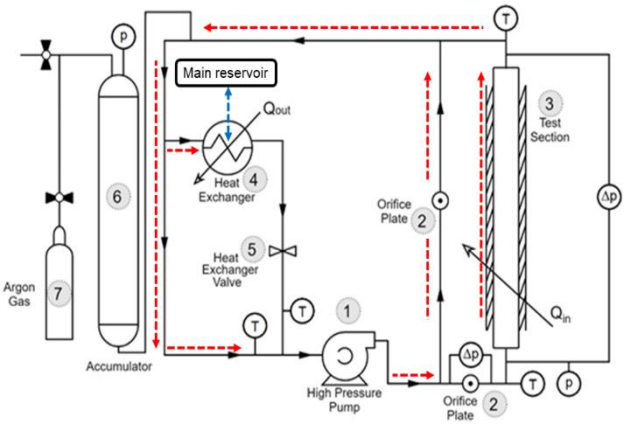

Figure 1. Schematics of high-pressure flow boiling facility located in University of Wisconsin-Madison [3].

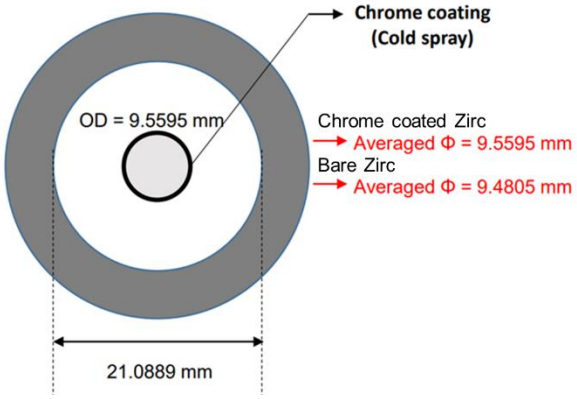

Figure 2 Schematics of the cross-section of the flow channel and heater rods with and w/o chromium coating

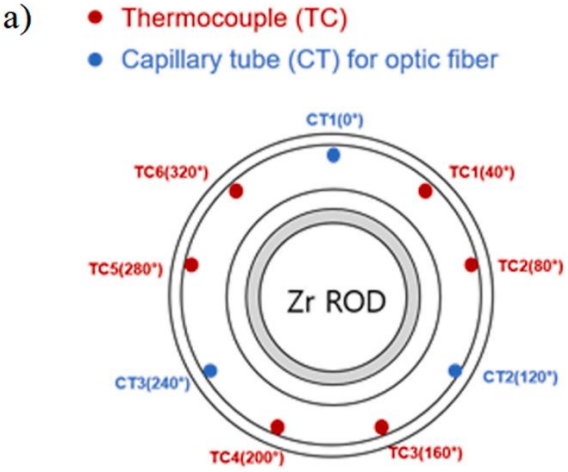

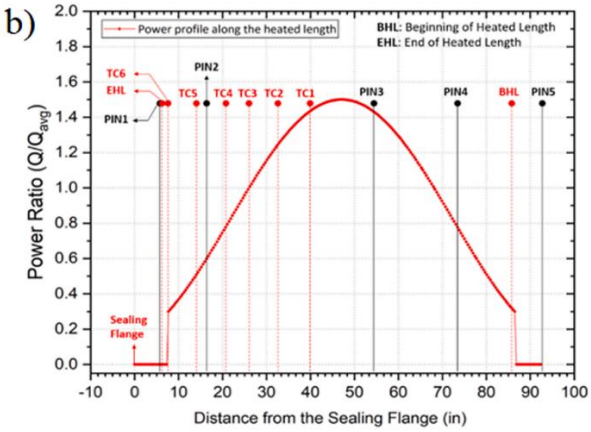

Figure 3 (a) Schematic of radial location of thermocouples and capillary tube for the optical fiber sensor. (b) The details of thermocouples and capillary tube location [3].

consists of a primary loop and a secondary loop. Those double loop systems can be seen in Fig. 1. The red arrows represent the primary flow path, and the blue arrow shows the secondary flow path. The working fluid (DI water, 4 MΩ resistance) flows through the test section and bypass channel with an installed orifice for the primary loop. Those flows recombine after the test section and part of this flows passes the main heat exchanger to cool do The rest of the flow bypasses the

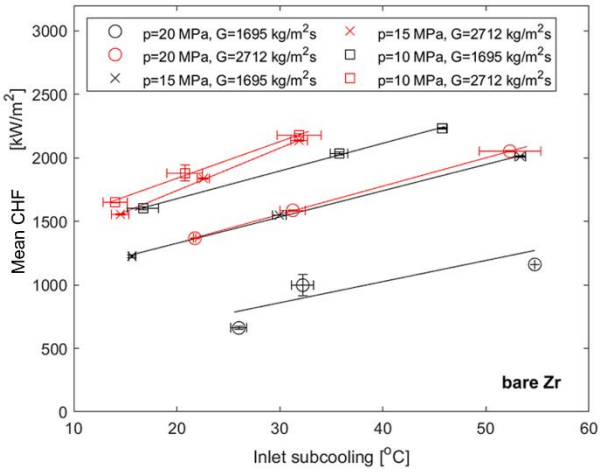

Figure 4 CHF results on bare Zr under various pressure, subcooling and mass flux conditions [3].

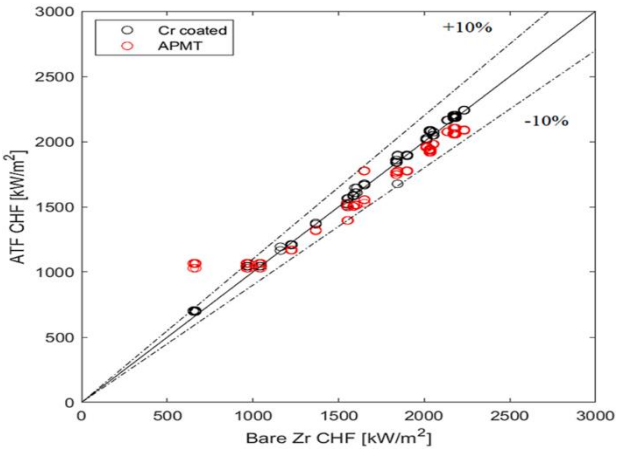

Figure 5 CHF comparison results between bare Zr and ATF materials (Cr coated Zr, APMT) [3].

main heat exchanger. The amount of flow that passes through the main heat exchanger can be controlled by the heat exchanger-bypass valve. The flows from the main heat exchanger recombine the heat exchanger-bypass flow and then flow into the high-pressure pump (Chem Pump GT series) together. The accumulator tank behind the flow loop receives the fluid's thermal expansion, which is connected to the Ar gas cylinder (6000 psi) to pressurize the system. The secondary loop is connected to the main reservoir to supply the coolant water to the main heat exchanger. Figure 2 shows the schematics of the cross-section of the flow channel and heater rods with and w/o chromium coating. It is found that the coating thickness was 150~200 um so we considered that coating thickness when we calculate the flow area and mass flux. The UW high-pressure flow boiling heat transfer loop can reach a maximum of 500-3500 kg/m²s, 25 MPa, and 400° C. The Stern heater rod can offer a maximum of 140 kW power and the flow channel was the annular shape with the single heater rod.

2.2 Thermocouple and capillary tube location

The 6 thermocouples and 3 capillary tubes for optical fiber were installed in the Stern heater rod to trip the CHF

and measure the temperature profiles with different radial directions. Prior to determining the TC location in the Stern heater rod, the predicted CHF location was investigated in the UW. The results showed that most of the desired CHF testing cases have the CHF occur just downstream of the center, so the TC locations are based on CHF results. The detailed information on the TC location and capillary tubes for optical fiber sensors with radial and axial direction is shown in Fig. 3(a) and (b),

2.3 CHF trip methods

The first CHF trip method is the temperature peak (~50ºC) trip using the thermocouple with the high-speed module (*NI SCB-68)* and the second is the current trip using the SCR software. TCs for the CHF trip was to measure the temperature with the 1 kHz and set up the trip setpoint for each thermocouple at every power step. In detail, we set up the trip setpoint to have 50ºC higher than the steady-state condition of each thermocouple. (e.g., 500ºC steady state, 550ºC trip setpoint) This is because we confirmed that ~50ºC temperature peak occurred at the prototypic PWR conditions in the previous CHF testing results [4-6]. The maximum cladding temperature was ~650ºC according to calculation since the core temperature will go up to 1200ºC (the Inconel ribbon coil can be damaged at ~1200ºC) at this condition. To avoid touching the 650ºC cladding temperature, we set up the 30~40ºC CHF trip temperature when the steady-state temperature goes up to 550ºC. The Stern heater rods were not damaged severely after all CHF testing. The reason for this is as follows: a. The cartridge heater has a high thermal mass so that it can spread the heat at the CHF to hold up the high temperature [7]. b. The vapor film at CHF was suppressed owing to the high-pressure conditions to simulate the PWR.

2.4 CHF Testing Procedure

The desired conditions (pressure, inlet temperature, mass flux) should be set up near the predicted CHF power for the CHF testing. Since the pressure is increased as the temperature increases, we set up the initial loop pressure 2~3 MPa below the desired pressure then adjust the pressure near the CHF. The Stern heater rod is the only heat source in the high-pressure flow loop. The inlet temperature can be controlled by adjusting the amount of exchanged heat at the main heat exchanger. The amount of water flow to the main heat exchanger can be controlled by adjusting the heat exchanger-bypass valve. The mass flux can be adjusted by controlling the RPM of the high-pressure pump. Prior to CHF testing, the proper bore size of the orifice plate should be installed by considering the desired mass flux. Also, the performance degradation of the high-pressure pump should be considered when we design the orifice bore size. This study used the 0.45" bore size orifice to reach the mass flux of 1695 kg/m^{2}s to 2720 kg/m^{2}s for the CHF testing. The CHF testing procedure is as follows: The power can be increased with a 1 kW step size at 30%

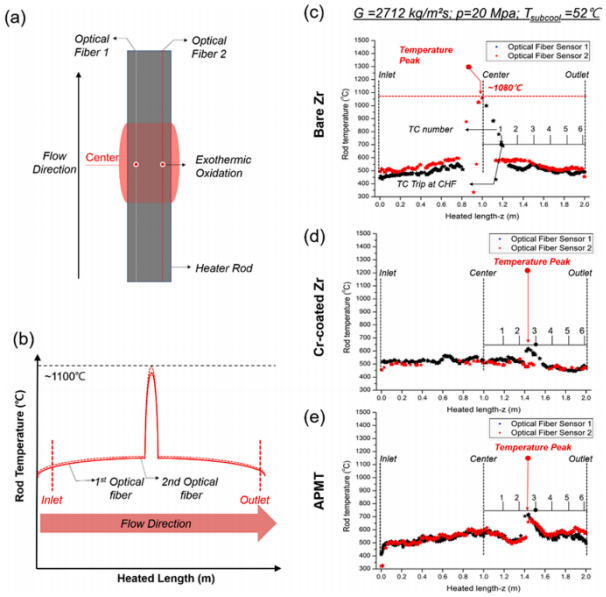

Figure 6. Schematic of the a) DNB event with the exothermic oxidation and b) predicted temperature profile when using the optical fibers. The temperature profiles obtained by the optical fibers on the c) bare Zr, d) Cr coated, and e) APMT under the same severe conditions (highest subcooling, pressure and mass flux conditions) [3].

below the predicted CHF power. Prior to increasing the power, the steady-state condition of the flow should be secured in the loop. We confirmed the steady-state condition when the inlet temperature fluctuation range was within the 0.2ºC. This normally took over 10 minutes at each power step. From 20% to 10% below the CHF, the power can be increased with a 0.5 kW step size. Then from 10% below the CHF, the power was increased by 0.1 kW until the CHF reached.

2.5 Optical Fiber Description

The three optical fibers were installed with the same radial spacing (120°) in the capillary tubes. Each optical fiber measured the temperature profile at the CHF occurrence location along the heated length. The temperature peak was detected at the CHF occurrence with the high-speed mode of the ODiSi module (100 Hz, 2.5 mm spacing gage setup) to evaluate the accurate CHF location. The optical fiber sensor setup details are in the published papers at UW-Madison [1,8,9].

3. Conclusions

Figure 4 shows the CHF results on the Zr cladding under various pressure, subcooling, and mass flux conditions. CHFs were enhanced as subcooling and mass flux rise, then CHFs were reduced as pressure rise. Cr-coated Zr and APMT alloys also showed the same tendency of CHF change with Zr as subcooling, mass flux, and pressure rise. Figure 5 shows the CHF comparison results between Zr and ATF materials. The CHF values were well matched within the 10% between Zr and ATF materials (Cr-coated Zr and APMT), so we

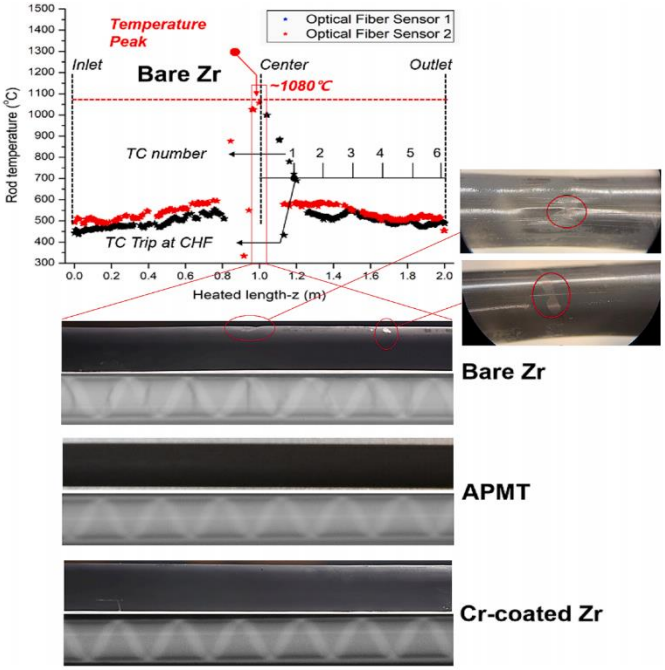

Figure 7. X-ray images at the center region of the heater for Bare Zr, Cr-coated Zr, and APMT. The Inset graph and image show the temperature profile measured by optical fiber on bare Zr and photographs at the heater-center under severe conditions [3].

confirmed that CHF was not significantly changed within 10% on the ATF materials (Cr-coated Zr and APMT) compared to Zr. Figure 6 (a)~(e) shows the schematic of the DNB event and measured temperature profile when using the optical fibers on the bare Zr, Cr coated, and APMT under the same conditions (harshest conditions: G=2712 kg/m^{2}s, P=20 MPa, $T_{subcool}$=52°C). From Fig 6 (a)~(e), we confirmed that although Cr-coated Zr and APMT maintained a fairly uniform temperature profile with a small temperature peak (650~680 °C) at CHF even at the harshest condition, bare Zr showed not uniform temperature profile with large temperature peak (~1100°C) at CHF at the same condition (harshest conditions: G=2712 kg/m^{2}s, P=20 MPa, $T_{subcool}$=52°C). After CHF testing, although ATF showed the normal optical fiber signal along the heater rod, Zr showed the failed optical fiber signal at the center of the heater rod. From those results, we inferred that the Zr cladding was damaged from CHF testing due to its high surface temperature (~1100°C, i.e. near the exothermic oxidation temperature) under the harshest condition. To understand the surface failure on Zr under the harshest condition, we conducted the surface inspection using an optical microscope to observe the surface damage after the CHF tests on the Zr and ATF materials (Cr-coated Zr and APMT). As we expected, ATF materials were not damaged after the CHF tests, meanwhile, Zr was damaged after the CHF tests due to an exothermic reaction of bare Zr induced by high surface temperature (~1100°C) under the severe DNB conditions (G=2712 kg/m^{2}s, P=20 MPa, $T_{subcool}$=52°C). We can confirm those facts through X-ray imaging. As shown in Fig. 7, X-ray imaging was performed to investigate the reason for surface damage. From the X-ray image, although no cracks were observed on the ATF material, a small crack (black solid line at X-ray image) was only observed on the Zr surface, so we inferred that it was made by penetration of the oxidized Zr layer (ZnO_2) at DNB. In conclusion, we demonstrated that Zr cannot prevent surface damage from the exothermic reaction at DNB under harsh DNB conditions whereas ATF cladding can safely prevent surface damage even at the harsh DNB conditions.

Acknowledgment

This work was partly supported by the National Research Foundation of Korea(NRF) grant funded by the Korea government(MSIT) (No. RS-2022-00166991)

REFERENCES

[1] Lee, D. et al. Enhanced flow boiling heat transfer on chromium coated zircaloy-4 using cold spray technique for accident tolerant fuel (ATF) materials. Appl. Therm. Eng. 185, 116347 (2021).
[2] Jo HJ, Yeom H, Gutierrez E, Sridharan K, Corradini M. Evaluation of critical heat flux of ATF candidate coating materials in pool boiling. Nucl Eng Des 2019;354. https://doi.org/10.1016/J.NUCENGDES.2019.110166.
[3] Moreira, T. A., Lee, D. H. & Anderson, M. H. Critical heat flux on zircaloy and accident tolerant fuel cladding under prototypical conditions of pressurized and boiling water reactors. Appl. Therm. Eng. 213, 118740 (2022).
[4] Lyons, K., Lee, D. & Anderson, M. Experimental study for critical heat flux in 2x2 rod bundles at high pressure conditions. Nucl. Eng. Des. 365, 110730 (2020).
[5] Greenwood, M. S., Duarte, J. P. & Corradini, M. Presentation and comparison of experimental critical heat flux data at conditions prototypical of light water small modular reactors. Nucl. Eng. Des. 317, 220–231 (2017).
[6] Duarte, J. P., Zhao, D., Jo, H. & Corradini, M. L. Critical heat flux experiments and a post-CHF heat transfer analysis using 2D inverse heat transfer. Nucl. Eng. Des. 337, 17–26 (2018).
[7] Stern Laboratories Inspection Report, IR-949-20 R1 Van Lochem, November 2020.
[8] Becker, K. F. & Anderson, M. H. Optical Fiber-Based Level Sensor for High Temperature Applications. IEEE Sens. J. 20, 9187–9195 (2020).
[9] Schneider, J. & Anderson, M. Using optical fibers to examine thermal mixing of liquid sodium in a pool-type geometry. Int. J. Heat Mass Transf. 158, 119968 (2020).